Multi-Dimensional K-Factor Analysis for V2V Radio Channels in Open Sub-urban Street Crossings

Laura Bernadó[1], Thomas Zemen[1], Johan Karedal[2], Alexander Paier[3], Andreas Thiel[4], Oliver Klemp[4], Nicolai Czink[1], Fredrik Tufvesson[2], Andreas F. Molisch[5], Christoph F. Mecklenbräuker[3]

[1]Forschungszentrum Telekommunikation Wien (FTW), Vienna, Austria
[2]Department of Electrical and Information Technology, Lund University, Lund, Sweden
[3]Institut für Nachrichtentechnik und Hochfrequenztechnik, Technische Universität Wien, Vienna, Austria
[4]Delphi Delco Electronics Europe GmbH, Bad Salzdetfurth, Germany
[5]Department of Electrical Engineering, University of Southern California, Los Angeles, CA, USA
Contact: bernado@ftw.at

***Abstract*—In this paper we analyze the Ricean K-factor for vehicle-to-vehicle (V2V) communications in a typical open sub-urban street crossing. The channel conditions vary from non line-of sight (NLOS) to line-of-sight (LOS). The antenna arrays used for recording the radio channels consist of 4 elements with directional radiation patterns. We measured 16 individual single-input single-output channels, with a bandwidth of 240 MHz for a duration of 20 s. We performed two kind of evaluations. For the first analysis we partitioned the 240 MHz bandwidth into 24 sub-bands with 10 MHz each, according to 802.11p. The small-scale fading of the first delay bin is Ricean distributed with a time-varying K-factor. The later delay bins are mostly Rayleigh distributed. We observe that the large/small K-factor values are not necessarily correlated with the received power. We show that the K-factor can not be assumed to be constant in time, frequency, and space. The antenna radiation patterns, and the illuminated objects by them at different time instances are the cause of these variations. The second evaluation considers the 240 MHz bandwidth, and the narrow-band K-factor is calculated for each frequency bin, with $\Delta f = 312$ kHz. We corroborate the need to consider the frequency variation of the K-factor. We conclude that a multi-dimensional varying K-factor models the large-scale statistical behaviour more accurately than a constant K-factor.**

I. Introduction

In wireless communication systems, small-scale fading statistics have a large impact on the performance of a communication link. The received signal consists of a deterministic component, and random components. The K-factor is defined as the ratio of the energy of the deterministic and the random part of the signal, and it is an indicator of the severity of the fading. A K-factor value close to 0 indicates strong fading (Rayleigh distributed), and a large K-factor value is related to less variations (Ricean distributed). It is a common approach in wireless communication systems to describe the distribution of the amplitude of the channel coefficient with the K-factor of a Ricean distribution.

This research was supported by the FTW project COCOMINT funded by Vienna Science and Technology Fund (WWTF), as well as the EC under the FP7 Network of Excellence projects NEWCOM++. The Telecommunications Research Center Vienna (FTW) is supported by the Austrian Government and the City of Vienna within the competence center program COMET.

For testing and simulation purposes the assumption of a constant K-factor is widely used. However, in mobile communications there are several factors that could introduce variability to the K-factor. Therefore, we propose to extend the small-scale fading model by a time-/frequency-/space-varying K-factor to make the model comply with large-scale statistics.

There are few investigations regarding those variations [1], [2]. The authors in [1] develop an empirical model for time-varying Ricean fading. The model is based on measurements taken at 1.9 GHz with a bandwidth of 1.23 MHz. A dense urban environment with a cellular setting scenario is considered. In [2] a cellular setting is also considered. The same carrier frequency is used but with a bandwidth of 9 MHz. This allowed the authors to analyze time and frequency variability of the K-factor. It was found that the K-factor remains more or less constant over frequency.

Investigations on the small-scale fading statistics have also been carried out for vehicular communications at the 5 GHz frequency band [3], [4], [5], [6], [7]. It is a general finding that the amplitude of the first delay bin follows a Ricean distribution. In [3], [7], vehicle-to-vehicle (V2V) communications are considered for a highway scenario. Urban scenario results are presented in [4], [5], [6] but always considering two cars driving one after the other. None of these contributions describes the variability of the K-factor.

II. Measurement Data Description

In this section we describe the parameters of the data. The parameters relate to the instrumentation settings and the scenario where the measurement was performed.

A. Collected Measurement Data

The data used in this paper was collected during a measurement campaign named DRIVEWAY'09 [8] conducted in Lund, Sweden, in June 2009. For this investigation, we consider the 4×4 multiple-input multiple-output (MIMO) measurement setting. The selected carrier frequency is 5.6 GHz, close enough to the one dedicated for IEEE 802.11p deployment. The measured bandwidth covers a total of 240 MHz in 769 frequency bins with a frequency separation $\Delta f = 312$ kHz.

A measurement run consists of $S = 65535$ snapshots at a repetition time of $t_{rep} = 307.2\mu$ s resulting in a total measured time of 20 s.

The 802.11p standard dedicated to vehicular communications defines a carrier frequency of 5.9 GHz in a 10 MHz bandwidth OFDM modulation scheme. In order to obtain meaningful results for V2V systems, we split our measurement data. We consider $L = 16$ individual single-input single-output (SISO) channels and $Q = 24$ frequency sub-bands of 10 MHz bandwidth each. Table I summarizes the measurement parameters and the chosen parameters for estimation of the small-scale fading statistics.

TABLE I
PARAMETERS FOR MEASUREMENT AND FOR K-FACTOR ANALYSIS.

Parameters	Measurement	Analysis
Channels:	4×4 MIMO	16 SISO
Carrier frequency:	5.6 GHz	5.6 GHz
Measurement bandwidth:	240 MHz	24×10 MHz
Snapshot repetition time:	307.2 μs	307.2 μs
Recording time:	20 s	20 s

The transmitter (Tx) and receiver (Rx) parts of the channel sounder are mounted into two cars. Each car is equipped with 4 circular patch antennas mounted in a linear array perpendicular to the driving direction. The antennas have a main lobe that covers the 4 main propagation directions, respectively, to the front, to the back, and to both sides of the car [9].

The selected parameters for investigation provide K-factor results for 16 different channels, each channel contains 24 different 10 MHz frequency sub-bands. Each sub-band is measured for a time duration of 20 s. With these available data we can conduct space-frequency-time K-factor analysis.

The time and frequency analysis in Section IV is focused mainly on link 10, Tx element 3 to Rx element 3, the radiation pattern of the corresponding antenna elements 3 are shown in Fig. 1. Figure 2 shows an schematic view of the orientation of the radiation patterns for the Tx and the Rx, and Tab. II shows the mapping between the links and the antenna elements.

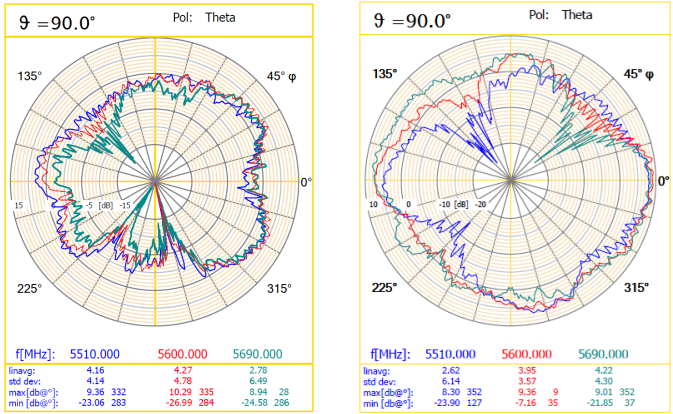

(a) Radiation pattern Tx antenna 3. (b) Radiation pattern Rx antenna 3.

Fig. 1. Radiation pattern of antenna element 3, 0° shows the driving direction.

TABLE II
LINKS AND CORRESPONDING TX-RX ANTENNA PAIRS.

link	Tx ant.	Rx ant.	link	Tx ant.	Rx ant.
1	1	4	9	3	4
2	1	3	10	3	3
3	1	2	11	3	2
4	1	1	12	3	1
5	2	4	13	4	4
6	2	3	14	4	3
7	2	2	15	4	2
8	2	1	16	4	1

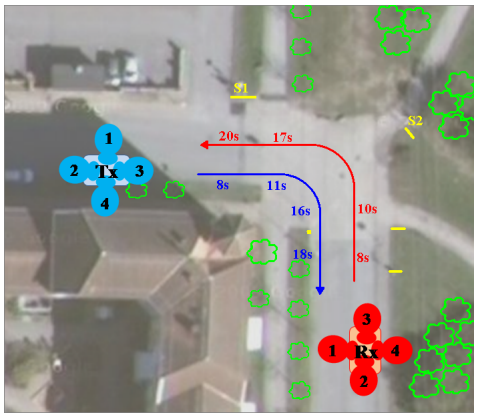

Fig. 2. Scenario layout. Position of trees, traffic signs and car trajectories.

B. Measurement Scenario

The selected scenario for this investigation is depicted in Fig. 2. The Tx and the Rx cars approach a sub-urban open crossing. There are only buildings in one of the quadrants of the intersection, which causes a non line-of-sight (NLOS) communication between Tx and Rx when the cars are far away from each other. During the measurement run there is a transition between NLOS and LOS situation. In the other 3 quadrants there are trees and other far buildings. The measurements were taken with light wind.

The two cars describe a parallel trajectory, they approach the crossing and turn right/left respectively, as indicated in Fig. 2 in blue for the Tx and red for the Rx. They are in LOS situation when they both are right at the crossing, between 11 and 16 s. The drivers are able to establish visual contact with the other car at 8 s. The Tx leaves the crossing at 18 s, the Rx does it at 20 s. The colored numbers in Fig. 2 show the position at which the Tx (blue) and the Rx (red) are at the time given by the number.

III. K-FACTOR ESTIMATION

In order to perform the small-scale fading analysis of the measured data, we need to conduct some pre-processing. This pre-processing consists of searching for the delay bins corresponding to the first strong path in the impulse response (IR), and shift it to the origin. This is done on a per link, per frequency sub-band, and per time instance basis. The delay resolution of each IR is 0.1 μs.

We first have a look at the per-delay-bin small-scale fading distribution. To do that, we select a link, a frequency sub-band and a time instance. We estimate the K-factor by using

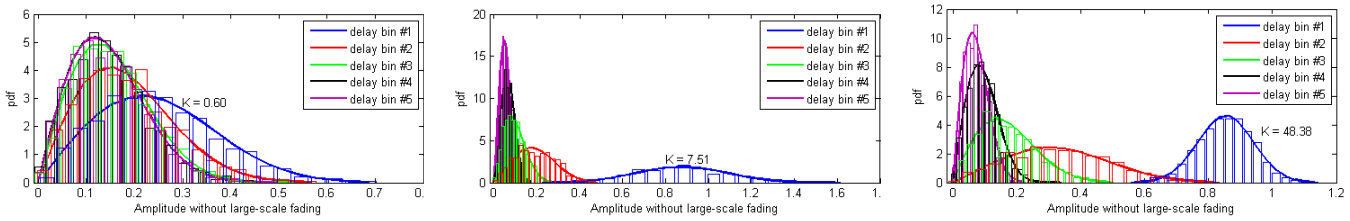

(a) t=6.5 s (b) t=11.5 s (c) t=17.5 s

Fig. 3. Fitted pdf and histogram for 1-5 delay bins for link 10 and frequency sub-band 1 at three different time instances using a sample size of 1500 samples

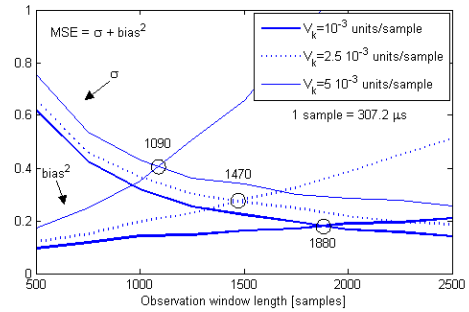

Fig. 4. Bias^2 and variance of the K-factor estimator for three K-factor variation velocities.

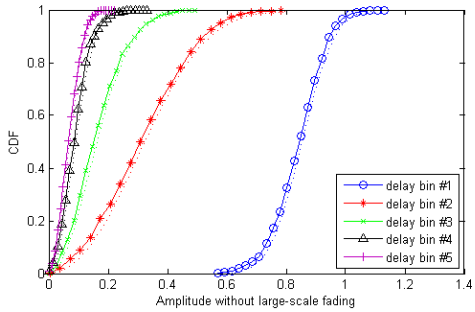

Fig. 5. CDF for 1-5 delay bins for link 10 and sub-band 1 at 17.5 s using a sample size of 1500 samples.

the method of moments (MoM) [10] that provides us with a first guess. Then we apply a least squares (LS) fit of the Rice distribution curve to the data histogram so that the mean-square-error (MSE) between the empirical and the analytical cumulative density function (CDF) is minimized. The MoM estimator fits the first and second order moments of the data in order to derive the K-factor, with the LS fit estimator, the shape of the Ricean distribution is fitted to the actual data [11]. We have tried out several sample lengths and corroborated that MoM and LS fit estimators deliver very similar results when considering an assemble larger than 1000 samples.

In order to select the sample size used for estimation, we have to take several aspects into account. First, the observation period can not exceed the stationarity length of the process. Second, a large number of samples has to be used in order to obtain meaningful statistical results.

In that sense we analyzed the performance of the estimator for different sample sizes in terms of variance and bias. We generate Ricean distributed channels analytically with a K-factor of 10, and add white Gaussian noise with a signal-to-noise ratio of 25 dB, which is the one observed in measurements. Since we assume that the K-factor changes in time, we test the estimator for three different K-variation speeds: 10^{-3}, $2.5{\cdot}10^{-3}$, and $5{\cdot}10^{-3}$ units/sample, which correspond to 3.25, 8.14, and 16.28 units/second respectively.

Figure 4 shows the bias^2 and the variance of the estimator for the different speeds. The intersection between the bias^2 and the variance curves sets the point at which the MSE is minimum, which is highlighted with a circle for the three cases.

In Fig. 4 we can observe the effects of the two important aspects we commented before. The observation window length achieving the minimum MSE decreases as the velocity increases. This also corroborates that the stationarity time is strongly dependent on the K-factor changes. Further, we observe that the minimum MSE increases when short window lengths are considered, i.e. the number of used samples for estimation is not sufficient to obtain a trustfully estimate.

Based on these conclusions, we select a sample size of 1500 snapshots. The samples are surrounding the selected time instance. With that, we assume that the process remains stationary within 0.46 s. In section IV-A we cross-check this result by calculating the mode of the velocity of change in the K-factor in the measurements, which results to be $2.32 \cdot 10^{-3}$ units/sample.

Figure 3 (a), (b), and (c) show the probability density function (pdf) of the first five delay bins of link 10, frequency sub-band 1 at time instances 6.5 s, 11.5 s, and 17.5 s respectively. At 6.5 s the two cars are approaching the crossing, they are in NLOS situation. At 11.5 s both are entering the crossing and they leave it at 17.5 s.

We can observe that delay bins 3-5 follow a Rayleigh distribution throughout the time instances. The second delay bin evolves from a Rayleigh to a Ricean distribution. On the other hand, the first delay bin appears to be clearly Ricean distributed with a varying K-factor for the three different time instances, $K_{t=6.5} = 0.60$, $K_{t=11.5} = 7.51$, and $K_{t=17.5} = 48.38$.

Both CDFs are depicted in Fig. 5 for link 10, frequency sub-band 1 at 17.5 s. The solid line corresponds to the CDF of the data and the dotted line to the empirical one calculated with the estimated K-factor, and they show a very good match.

IV. Space-Time-Frequency Varying Analysis for the First Delay Bin

We want to investigate the temporal, spatial (link-wise), and frequency dependency of the small-scale fading. We focus

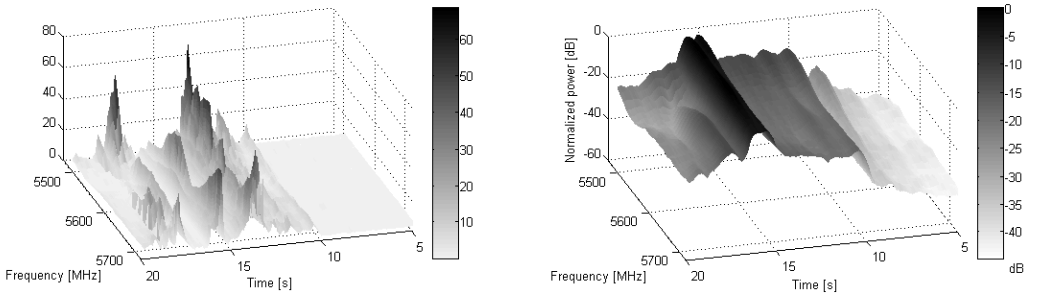

(a) Time-frequency (per sub-band) dependent K-factor. (b) Time-frequency (per sub-band) dependent power.

Fig. 6. Time-frequency dependent results for tap 1 of link 10.

on the first delay bin. Figure 6 shows a 3D representation of the K-factor for the first delay bin of link 10 next to its corresponding time-frequency power. We observe an evolution of the K-factor and the normalized power in both domains, frequency and time.

There is not necessarily a correspondence between received power and K-factor. Large K-factors are observed between 13 and 18 s. However, the estimated K-factor is small from 6 to 13 s, although the received power is not negligible. In that case, there is almost no deterministic part in the received signal and thus it is described by a Rayleigh distribution. On what follows, we discuss time, frequency, and space variability of the K-factor of the first delay bin independently.

A. Time-varying K-factor

We show the time evolution of the K-factor and received power for three different frequency sub-bands in Fig. 7. Although the K-factors do not present the same value, they show the same tendency.

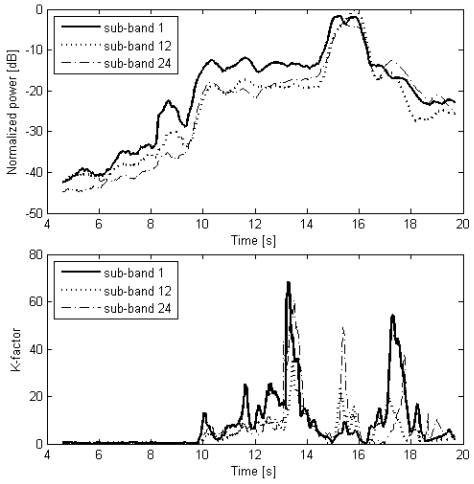

Fig. 7. Time-varying K-factor and power for link 10 and three different frequency sub-bands for a sample size of 1500.

At around 13.5 s the K-factor experiences an increase, in contrast to the received power which remains constant. To explain the variations in the received power we look at the radiation pattern of the antennas. The antennas do not have omni-directional radiation patterns and present a lower gain between 120 ° and 150 °, and between 180 ° and 210 ° with respect to the driving direction, with lower gain within the first sector (120 ° - 150 °), see Fig. 1. At 13.5 s, the first low-gain cones at 135 ° are aligned and the cars are very close to each other with no objects in between. At that point, the radiated power is not enough to reach further objects that could produce scattering, and the direct connection Tx-Rx predominates resulting in a large K-factor. At 17.5 s, the second low-gain sectors at 195 ° are aligned. At that point there is a tree and a street light relatively close to the straight line joining Tx and Rx, which can contribute with scattering and thus increasing the effect of the random components in the received signal.

B. Frequency-varying K-factor

We analyze now the frequency-varying behaviour of the K-factor. For that, we select three different time instances for link 10 and plot their K-factor as a function of the 24 frequency sub-bands in Fig. 8. We cannot necessaritly assume the same small fading statistics characteristics throughout a range of 240 MHz.

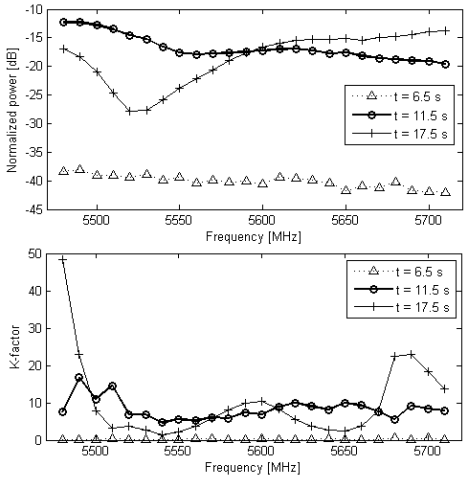

Fig. 8. Frequency-varying per sub-band K-factor and power of the first delay tap for link 10 and three different time instances.

This might be due to small reflecting elements contributing at different frequencies, such as foliage from the trees surrounding the road, or due to frequency dependent antenna

pattern that could especially influence the power of the dominating component. We observe different small-scale fading statistics throughout the 24 different frequency sub-bands.

Another cause of the frequency variation of the K-factor is the frequency dependent antenna pattern gains throughout the 240 MHz measurement bandwidth. As it can be observed in Fig. 1, the radiation pattern of elements Tx3 and Rx3 changes significantly at the lower, central, and upper band. This effect is mainly observed for Tx element 3, where the gain experiences an increase/decrease of 10 dB at the bandwidth edges with respect to the carrier frequency. Even though they do not lose the directionality, there are certain regions where deep dips appear, such as at 50°, and 280° for the Tx element 3. For the Rx element 3, the variations in frequency of the radiation pattern are not as severe as for the Tx element.

It is normally expected that the large-scale behaviour of the K-factor does not change within a narrow-band frequency bandwidth. In our case, the relative bandwidth of two consecutive frequency sub-bands, i.e. 20 MHz, is less than 10%. Therefore it is noteworthy the strong frequency variation of the K-factor already from sub-band to sub-band.

C. Space-varying K-factor

The K-factor is also different depending on the selected link between Tx and Rx antennas because we used directional antennas. We consider 4 of the 16 measured SISO channels, links 1, 7, 10, 16. Link 1 corresponds to a bad communication situation, where the antennas of the Tx and the Rx are facing towards the quadrants where there are no objects. Therefore, a sufficiently strong received signal may be obtained only very close to the crossing, almost when the two cars already see each other. On the other hand, link 10 consists of the Tx and Rx antennas with the radiation pattern oriented to the front. In that case it is more likely to have a sufficient signal strength before arriving to the crossing since we basically need diffraction. The additional reflection will not help getting the signal to reach the Rx before we have LOS. The complementary Tx-Rx antenna combination is given in link 7, where the antennas radiate towards the back side of the car. The last case we analyze here is link 16, which considers the two antennas of Tx and Rx having a radiation pattern oriented to the side of the road that has buildings.

Figure 9 shows the time-frequency dependent K-factor for the four described links.

Due to the orientation of the antenna radiation patterns and the position of trees and traffic signs (see Fig. 2), the time-frequency variation of the K-factor is different depending on the considered link. There is a big traffic sign (S1) parallel to the road at which the Rx antenna 4 is facing at 17 s. The K-factor for link 1 appears to be large at this time instance.

The effect of another traffic sign (S2) can be appreciated in link 7, when the two cars are leaving the crossing. The K-factor at that time is large due to a reflection of the signal on S2.

The Tx antenna 4 faces the inner part of the corner during the whole measurement run. On this side of the street there are

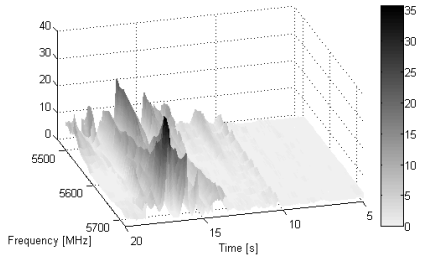

(a) link 1

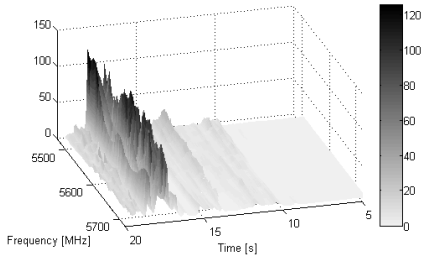

(b) link 7

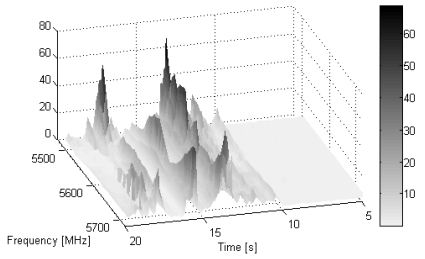

(c) link 10

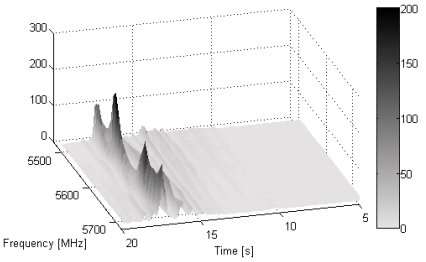

(d) link 16

Fig. 9. Time-frequency dependent K-factor for four different links.

trees. When we look at link 16, the Rx antenna is also facing the same part of the street. Therefore, the largest K-factor is observed at about 17.5 s, when the Rx car benefits from the influence of the large street sign, present on the other side of the road.

For these 3 links (1, 7, and 16), the frequency variation is not as severe as for link 10, where the influence of the trees seems to be more important.

V. Narrow-band K-factor

We observed a strong frequency dependability of the K-factor in the analysis performed in Sec. IV-B. Since the IEEE 802.11p standard is OFDM based, this frequency variability will have an influence on the communication system per-

formance. Therefore, we look now into the time-frequency variation of the narrow-band K-factor.

We proceed with the estimation of the K-factor in the frequency domain instead of in the delay domain, as it was done in the previous section. In that case, we do not separate the frequencies in sub-bands. The K-factor is estimated per frequency bin for the whole bandwidth of $240\,\text{MHz}$ with a frequency resolution of $\Delta f = 312\,\text{kHz}$ and using a sample size of 1500 snapshots.

The upper plot in Fig. 10 shows a 2D representation of the time-frequency dependence of the K-factor for link 10. The explanation of the variation in time is similar to the one given in Sec. IV-A. The increase and decrease of the K-factor depends on the interacting objects, and orientation of the cars, and the antenna patterns.

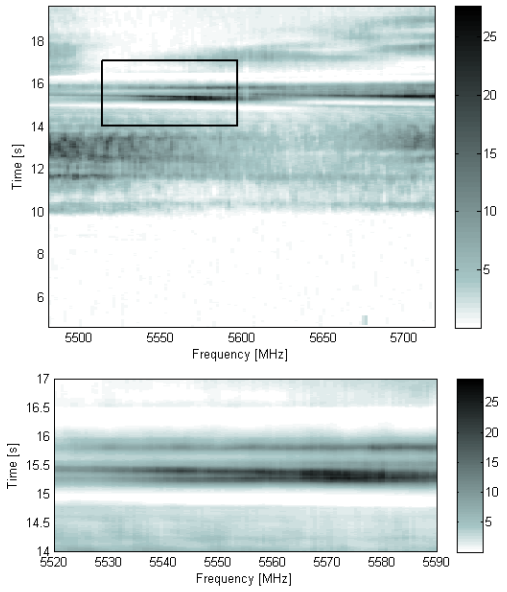

Fig. 10. Narrowband K-factor for link 10.

In the narrowband analysis we can also appreciate the frequency variation of the K-factor. From an OFDM system point of view, the fading affecting the different sub-carriers is different. On the bottom of Fig. 10 we see an enlarged portion of the upper plot, namely the one surrounded by a black square. The bandwidth in the 802.11p standard is $10\,\text{MHz}$, then we see 7 consecutive sub-bands. The frequency variation is also observed already within one sub-band.

VI. Conclusions and Outlook

We analyzed the per-delay-bin narrow-band small-scale fading statistics for vehicle-to-vehicle communication radio channels. We analyzed a set of measurement data where a single run consists of $20\,\text{s}$ of measurement time, 24 frequency sub-bands each of $10\,\text{MHz}$ bandwidth, and 16 different links. For each sub-band we found that the first delay bin is Ricean distributed with a varying K-factor, and the following delay bins are mostly Rayleigh distributed. We investigated the variability of the K-factor in the time, frequency (per sub-band), and spatial domain, and found that it is necessary to account for these variations. Since the communication system for vehicular communications is OFDM based, we also analyzed the K-factor on a per-frequency-bin basis. The narrow-band results show a different fading behaviour per sub-carrier, thus also supportting the results obtained in the delay domain. The K-factor changes dramatically depending on several factors: (*i*) Number of illuminated scatterers due to the antenna radiation pattern and objects in between Tx and Rx, (*ii*) the antenna radiation pattern changes over frequency, (*iii*) presence of good reflecting objects near the cars (traffic signs). The effect of the radiation pattern of a realistic vehicular antenna is important, since its characteristics will influence the K-factor a receiver will be able to estimate. Given these observations, a stochastic approach could be followed to model the multi-dimensional variability of the K-factor for such communication scenarios. Such a model is crucial for realistic link-level testing of future vehicular communication systems.

References

[1] G. G. Messier and J. A. Hartwell, "An Empirical Model for Nonstationary Ricean Fading," *Vehicular Technology, IEEE Transactions on*, vol. 58, no. 1, pp. 14–20, January 2009.

[2] L. J. Greenstein, S. Ghassemzadeh, V. Erceg, and D. G. Michelson, "Ricean K-Factors in Narrow-Band Fixed Wireless Channels: Theory, Experiments, and Statistical Models," *Vehicular Technology, IEEE Transactions on*, vol. 58, no. 8, pp. 4000–4012, October 2009.

[3] J. Karedal, F. Tufvesson, N. Czink, A. Paier, C. Dumard, T. Zemen, C. Mecklenbräuker, and A. Molisch, "A Geometry-Based Stochastic MIMO Model for Vehicle-to-Vehicle Communications," *Wireless Communications, IEEE Transactions on*, vol. 8, no. 7, pp. 3646–3657, July 2009.

[4] G. Acosta-Marum and M. A. Ingram, "Six Time- and Frequency-Selective Empirical Channel Models for Vehicular Wireless LANs," *IEEE Vehicular Technology Magazin*, pp. 4–11, December 2007.

[5] J. Maurer, T. Fügen, and W. Wiesbeck, "Narrow-Band Measurement and Analysis of the Inter-Vehicle Transmission Channel at 5.2 GHz," in *IEEE 55th Vehicular Technology Conference*, Birmingham, Alabama, USA, May 2002.

[6] L. Cheng, B. E. Henty, D. D. Stancil, F. Bai, and P. Mudalige, "Mobile Vehicle-to-Vehicle Narrow-Band Channel Measurements and Characterization of the 5.9 GHz Dedicated Short Range Communication (DSRC) Frequency Band," *Journal on Selected Areas in Communications, IEEE Transactions on*, vol. 25, no. 8, pp. 1501–1516, October 2007.

[7] O. Renaudin, V.-M. Kolmonen, P. Vainikainen, and C. Oestges, "Wideband MIMO Car-to-Car Radio Channel Measurements at 5.3 GHz," in *IEEE 68th Vehicular Technology Conference*, Calgary, Alberta, Canada, September 2008.

[8] A. Paier, L. Bernadó, J. Karedal, O. Klemp, and A. Kwoczek, "Overview of Vehicle-to-Vehicle Radio Channel Measurements for Collision Avoidance Applications," in *IEEE 71st Vehicular Technology Conference, to be presented*, Taipei, Taiwan, May 2010.

[9] O. Klemp, A. Thiel, A. Paier, L. Bernadó, J. Karedal, and A. Kwoczek, "In-situ vehicular antenna integration and design aspects for vehicle-to-vehicle communications," in *The 4th European Conference on Antennas and Propagation (Eucap 2010), to be presented*, Barcelona, Spain, April 2010.

[10] L. J. Greenstein, S. Michelson, D. G., and V. Erceg, "Moment-method estimation of the Ricean K-factor," vol. 3, no. 6, June 1999, pp. 175–176.

[11] C. Oestges, N. Czink, B. Bandemer, P. Castiglione, F. Kaltenberger, and A. J. Paulraj, "Experimental characterization and modeling of outdoor-to-indoor and indoor-to-indoor distributed channels," *Vehicular Technology, IEEE Transactions on*, vol. 59, no. 5, pp. 2253 –2265, jun 2010.